Supporting Information

Role for Metallothionein-3 in the Resistance of Human U87 Glioblastoma Cells to Temozolomide

Rosa Santangelo[#], Enrico Rizzarelli[§,∫], Agata Copani[#,∫,*]

[#]Department of Drug Sciences, University of Catania, 95125 Catania, Italy.
[§]Department of Chemical Sciences, University of Catania, 95125 Catania, Italy.
[∫]Institute of Crystallography, National Council of Research, 95125 Catania, Italy.

Corresponding author:

Agata Copani[*]

[*]acopani@katamail.com

Table S1. Primer sequences for Real-Time PCR analysis

Primer pairs	**Sequence**
MT1A	F, 5'-GTGCGCCTTATAGCCTCTCA-3' R, 5'-TCTCTGATGCCCCTTTGCAG-3'
MT1B	F, 5'-CTCCAGGCTTGTCTTGGCTC-3' R, 5'-CAGCGGCACTTCTCTGATGA-3'
MT1E	F, 5'-AGCATCCCCTTTGCTCGAAA-3' R, 5'-CACTTCTCCGATGCCCCTTT-3'
MT1F	F, 5'-CCTCCCCTGACTATCAAAGCA-3' R, 5'-TCTTCTTGCAGGAGGTGCAT-3'
MT1G	F, 5'-AACTCTAGTCTCGCCTCGGG-3' R, 5'-CAGGGCTGTCCCGACATCAG-3'
MT1X	F, 5'-TCTTGATCGGGAACTCCTGC-3' R, 5'-CTGCACTTGTCTGACGTCCC-3'
MT2A	F, 5'-AACCTGTCCCGACTCTAGCC-3' R, 5'-AGGAGCAGCAGCTTTTCTTGC-3'
MT3	F, 5'-CCAAGCGCACAAACGGAA-3' R, 5'-CAGGTCTCAGGGTCCATGTC-3'
ZIP4	F, 5'-CCTTCGCTGGTCTCTACGTG-3' R, 5'-CGGGTCCCGTACTTTCAACA-3'
ZnT1	F, 5'-CCTCGCGTTAAGAGCACCC-3' R, 5'-CAATTTCAGCCCGTTGGAGTT-3'
GAPDH	F, 5'-TGCACCACCAACTGCTTAGC-3' R, 5'-GGCATGGACTGTGGTCATGAG-3'

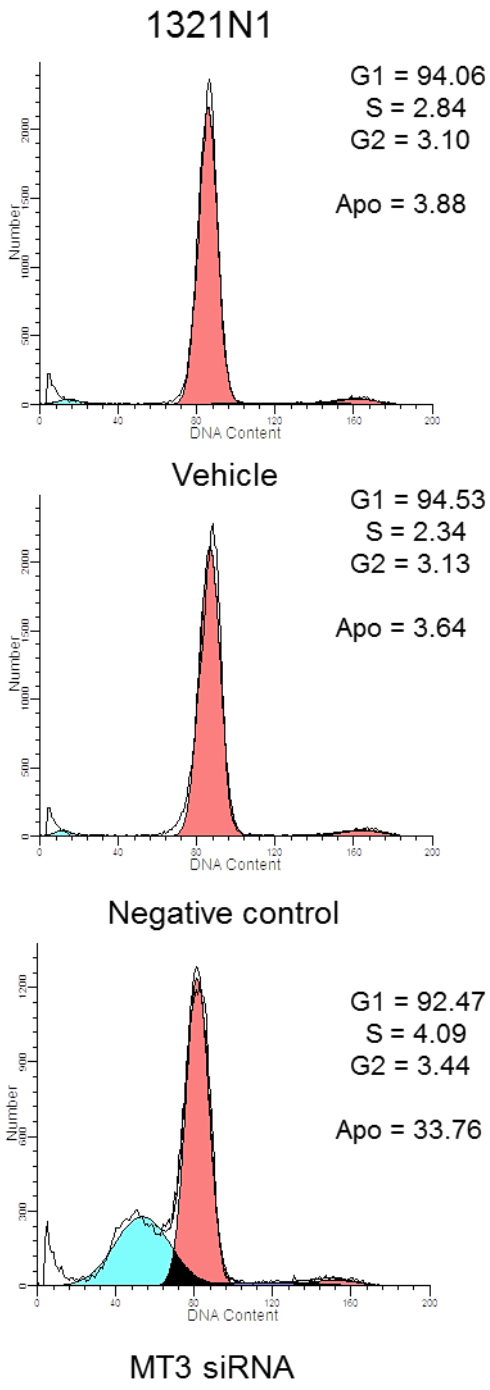

Figure S1. Representative histograms for apoptosis and cell cycle distribution profiles of 1321N1 cells treated with vehicle, negative control or MT3 siRNA as indicated. Percentage of G1, S and G2 cells are indicated in the legend. Apoptotic cells (% in the legend) are those distributed in the light blue area preceding the G1 peak. Note MT3 silencing-induced apoptosis of 1321N1 and the lack of effects of both vehicle and negative control.

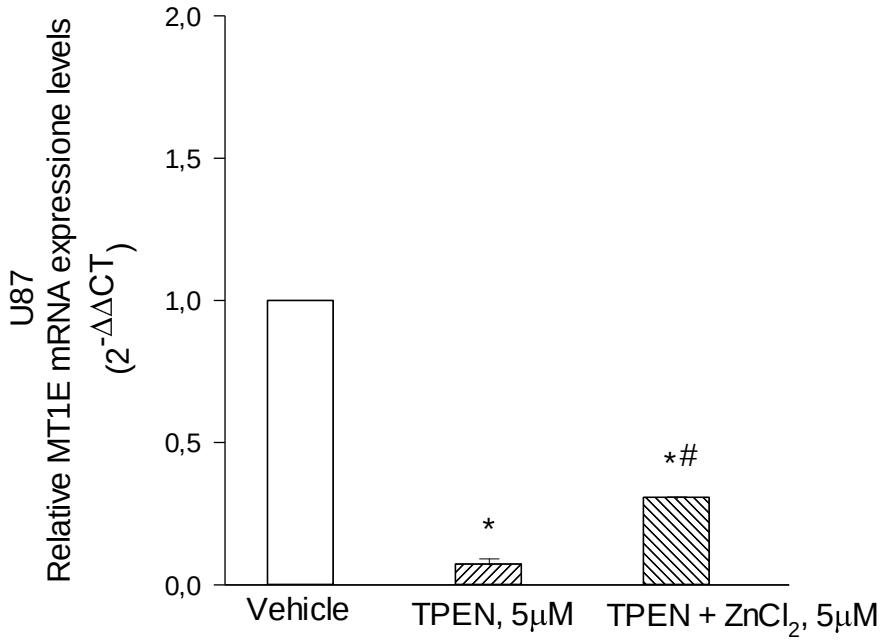

Figure S2. TPEN reduced MT1E mRNA expression in U87 cells, and the reduction was prevented in part by the addition of $ZnCl_2$. Bars represent the means ± SD from two distinct determinations, each performed in duplicate. *P< 0.05 vs. Vehicle and #p< 0.05 vs. TPEN alone.

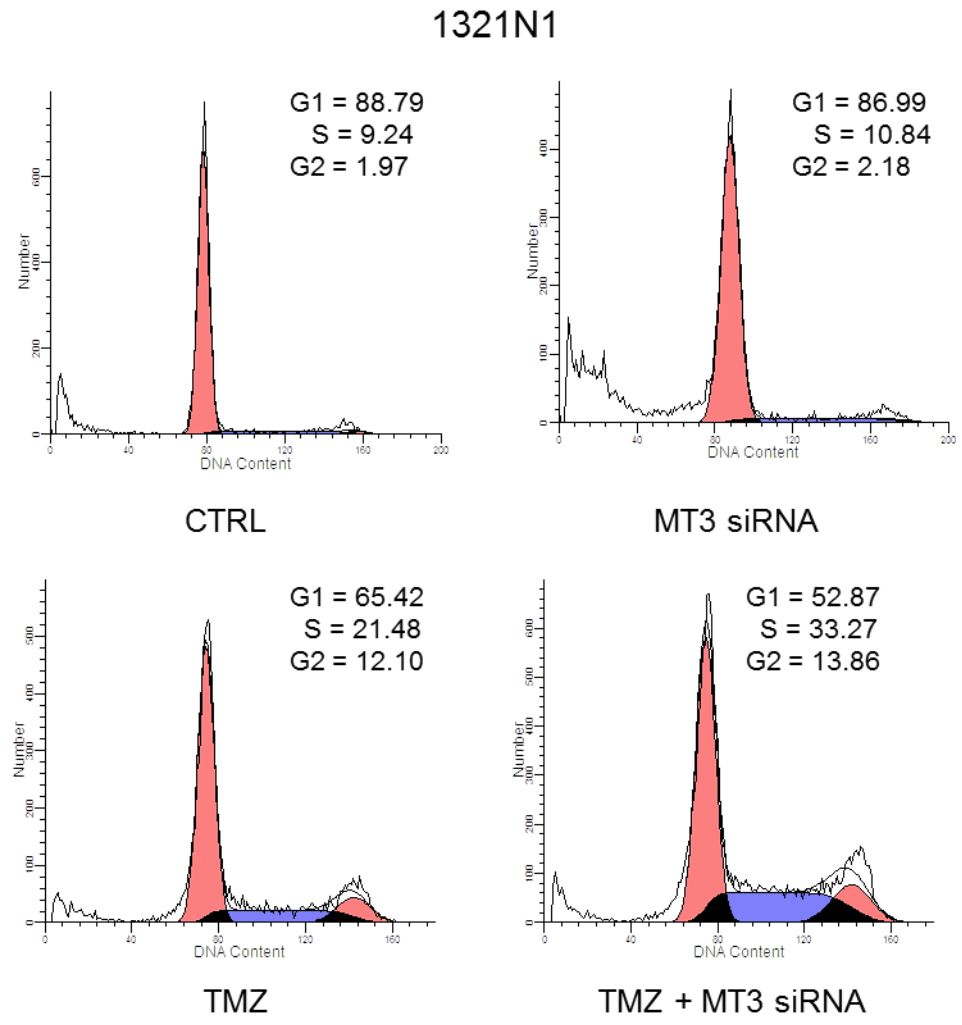

Figure S3A. Representative cell cycle distribution profiles of 1321N1 cells treated as indicated below the graphs. Percentages of G1, S and G2 cells are indicated in the legend. Note that TMZ produces a significant accumulation of S and G2 cells, and that MT3 silencing potentiates TMZ effects.

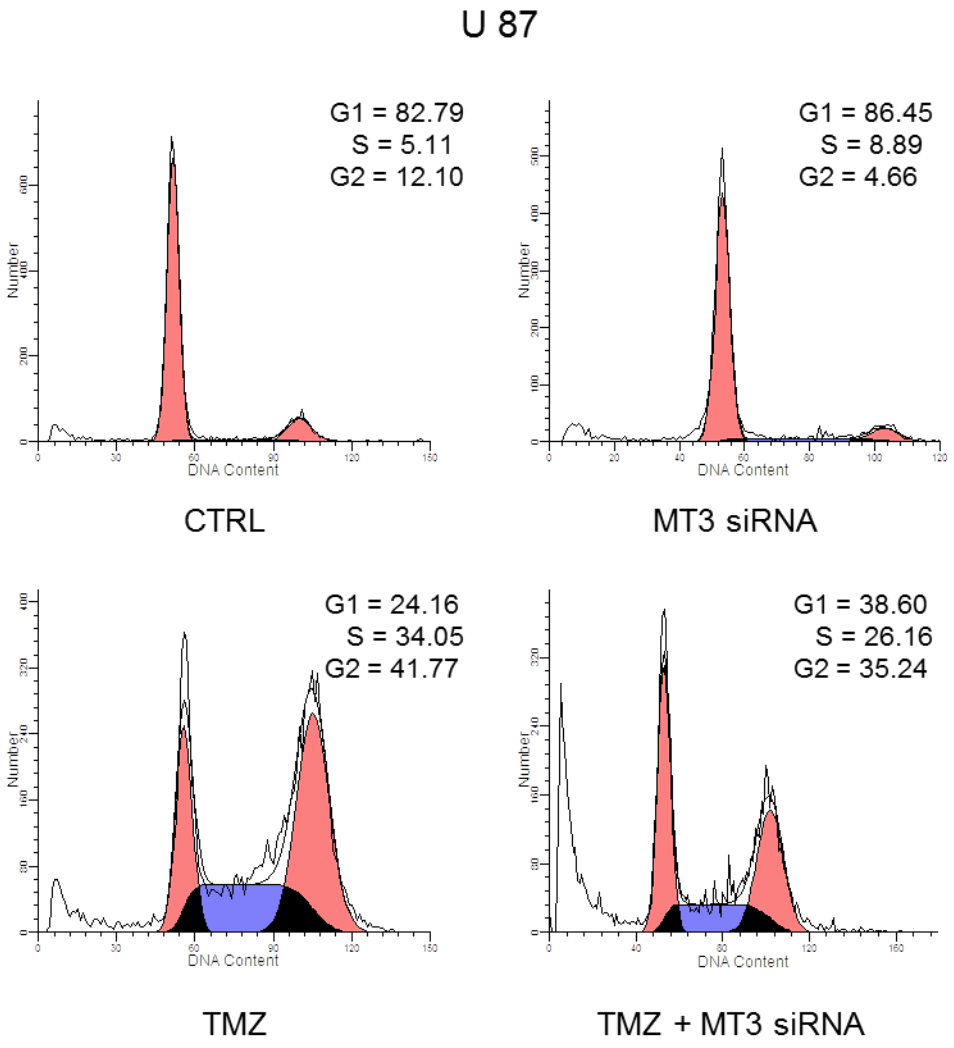

Figure S3B. Representative cell cycle distribution profiles of U87 cells treated as indicated below the graphs. Percentages of G1, S and G2 cells are indicated in the legend. Note the significant accumulation of S and G2 cells with TMZ alone, and the increased G1 population with TMZ+MT3 siRNA versus TMZ alone.

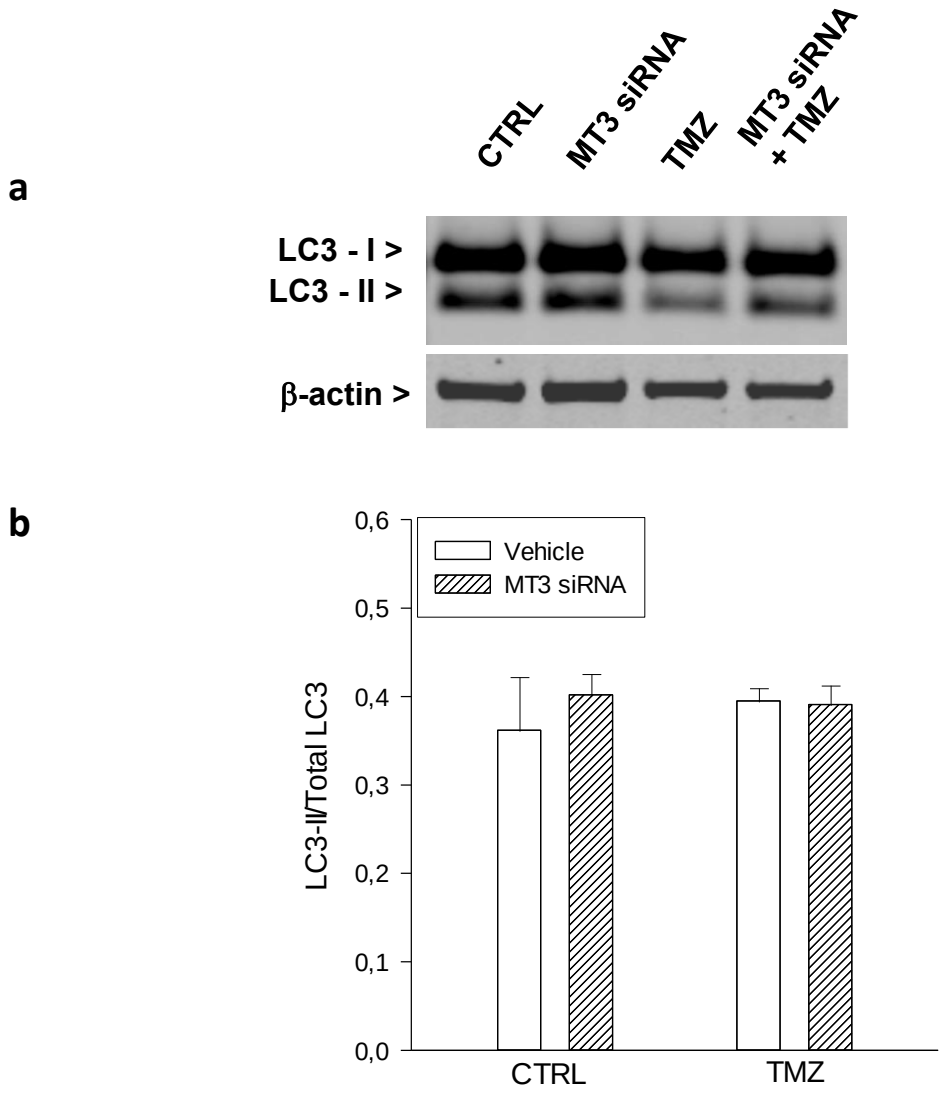

Figure S4. Western blot analysis of LC3 in U87 cells. The two bands, corresponding to the cytosolic LC-I and to the autophagosome-associated LC-II, are shown in (**a**). None of the treatments affected the band signals. The densitometric analysis of bands from two separate western blots is presented in (**b**). Both LC3-I and LC3-II signals were normalized against β-actin before the calculation of the LC3-II/Total LC3 ratio. Bars represent the means ± SD of 2 determinations.

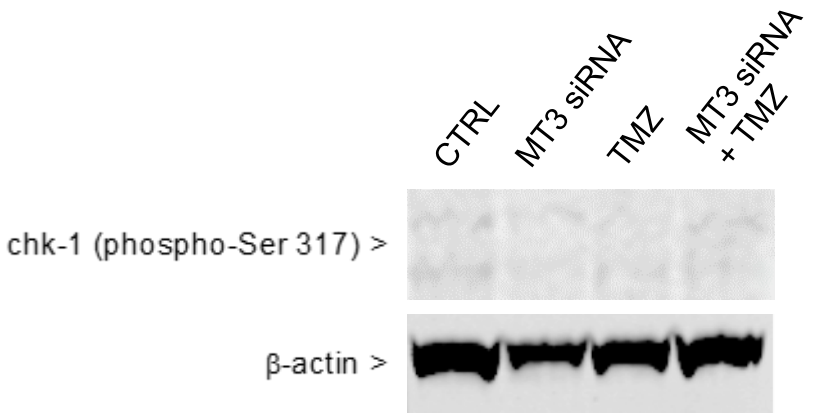

Figure S5. Western blot image of phosphorylated chk-1 at serine 317 and corresponding β–actin bands as a control for loading. Note that the chk-1(phospho-Ser 317) signal was barely visible under all conditions.

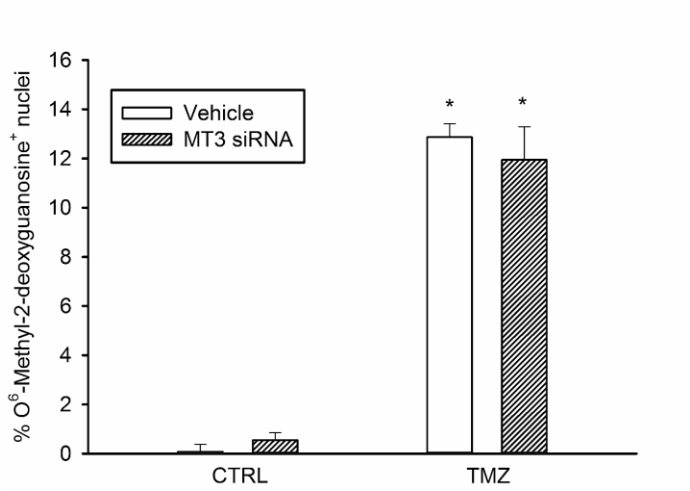

Figure S6. Flow cytometric analysis of isolated nuclei from U87 GBM cells following immunostaining for O6-methyl-2-deoxyguanosine. Bars represent the means ± SEM of four determinations. An average of 5000 nuclei/determination was counted. Note the significant percentage of immunopositive nuclei with TMZ (100 μM for 96 hours), which did not change with the addition of MT3 siRNA (5 nM for 96 hours). *P < 0.05 vs. the corresponding control (CTRL).